

Gd ESR IN UPt₃

R. Spitzfaden,^a A. Schütz,^a H.-A. Krug von Nidda,^a B. Elschner^a and A. Loidl^b

^aInstitut für Festkörperphysik, TH Darmstadt, D-64289 Darmstadt, Germany

^bExperimentalphysik V, Universität Augsburg, D-86135 Augsburg, Germany

1. INTRODUCTION

UBe₁₃ [1, 2] and UPt₃ [2] were the first heavy-fermion (HF) compounds that have been investigated by electron-spin resonance (ESR) techniques. HF metals reveal a Curie–Weiss susceptibility at high temperatures, but behave like Pauli-spin paramagnets below a characteristic temperature T^* , which is the Kondo-lattice temperature. For $T \ll T^*$, the metallic heat capacity and the magnetic susceptibility are strongly enhanced due to the formation of heavy quasiparticles [3, 4]. The high density of electronic states is a consequence of the strong hybridization of the almost localized $5f$ electrons with the band states. Using local probes, the density of states (DOS) at the Fermi energy can directly be measured using magnetic resonance techniques. It has been documented by Elschner and Loidl [5] that also ESR is a very useful tool to study the spin-dynamics in these materials. However, in the early ESR work on UBe₁₃ and UPt₃ no significant anomalies have been detected, neither in the g -values nor in the temperature dependence of the linewidth [1, 2]. These measurements on both compounds were performed in a narrow temperature range only and revealed no significant deviations to what would be expected for normal metals.

In this communication we present Gd-ESR data on UPt₃ in a wider temperature range. The temperature dependence of the linewidth reveals clear deviations from a Korringa behavior and shows the ESR characteristics of

other typical heavy-fermion systems [5], like CeCu₂Si₂ [6] or URu₂Si₂ [7].

2. EXPERIMENTAL RESULTS

UPt₃ crystallizes in the hexagonal Cd₃Mg structure ($P6_3/mmc$) with lattice constants $a = 5.72 \text{ \AA}$ and $c = 4.88 \text{ \AA}$. The symmetry of the uranium site is $\bar{6}m2$. The U–U distance amounts 4.1 \AA . From the low-temperature Sommerfeld coefficient ($\gamma \approx 0.4 \text{ J mol}^{-1} \text{ K}^{-2}$) a characteristic temperature of $T^* \approx 80 \text{ K}$ can be estimated [3], which yields a mass enhancement of the quasiparticles of approximately, $m^*/m_0 \approx 180$ [4]. For $T < 0.5 \text{ K}$ UPt₃ reveals superconductivity [8] coexisting with long-range antiferromagnetic order which is established at $T_N = 5 \text{ K}$ [9].

Polycrystalline UPt₃ samples were arc-melted in argon atmosphere using 99.7% purity uranium and high purity Pt doped with Gd. The samples were annealed for five days at 1173 K in an argon atmosphere. U_{1-x}Gd_xPt₃ samples with $x = 0.02$ and 0.005 were investigated. The ESR experiments were carried out in a conventional X-band (9 GHz) spectrometer. An Oxford continuous He-flow cryostat has been used for temperatures $T > 4.2 \text{ K}$ and a cold-finger bath cryostat for $T < 4.2 \text{ K}$.

To obtain single-crystal like behavior, the polycrystalline samples were powered to nearly single crystalline grains (diameter $\approx 40 \text{ \mu m}$) and immersed in paraffin. For orientation along the crystallographic c -axis

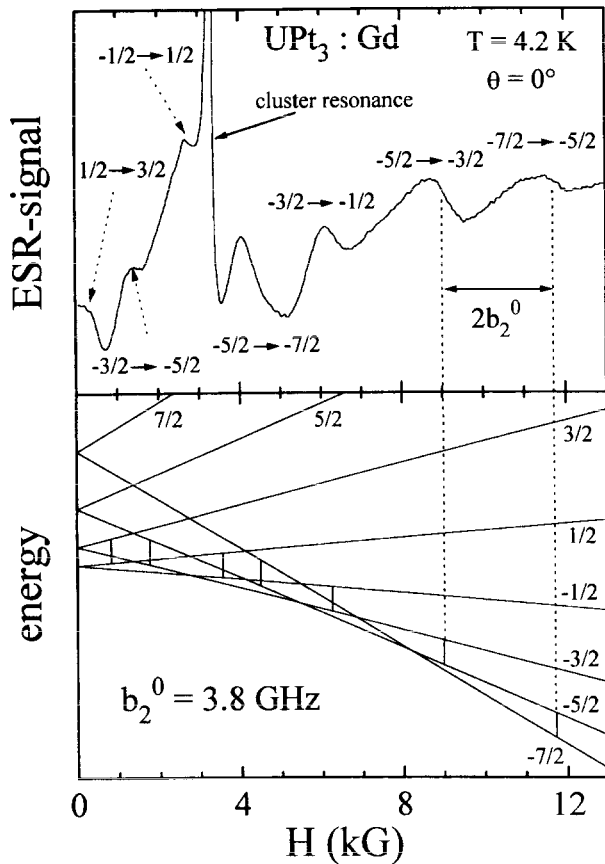


Fig. 1. Upper frame: ESR spectrum in UPt_3 doped with 2 at% Gd at 4.2 K. In this case the external field was parallel to the hexagonal c -axis of the grain-oriented powder. Lower frame: calculated energy levels of the Gd ground multiplet in an external magnetic field with an axial crystal field described by a CF parameter of $b_2^0 = 3.8$ GHz and magnetic dipole transitions for $\nu = 9.14$ GHz.

we applied a static magnetic field of 20 kG and rotated the sample around an axis perpendicular to the field while the paraffin was liquified. This rotation procedure described in [10] is necessary, because the magnetic susceptibility parallel to the c -axis is weaker than perpendicular to the c -axis in UPt_3 . Therefore the c -axis is adjusted perpendicular to the magnetic field along the rotation axis.

Contrary to what has been observed in CeCu_2Si_2 [6] and URu_2Si_2 for $T > T_N$ [7], no fully exchange-narrowed Gd spectrum has been observed in UPt_3 . Even at the highest temperatures and for the highest Gd concentrations a crystal-field split spectrum was detected. Figure 1 (upper frame) shows the absorption derivate of the ESR spectrum for 2 at% Gd in UPt_3 at $T = 4.2$ K and for the angle $\theta = 0^\circ$ between the c -axis of the grain-oriented samples and the external magnetic field \mathbf{H} . We tried to describe this well resolved fine-

structure spectrum using a spin Hamiltonian with a dominant uniaxial crystal-field contribution, neglecting higher terms as a first approximation for the hexagonal crystal-field symmetry [11]

$$H = \mu_B \mathbf{H} g \mathbf{S} + \frac{1}{3} b_2^0 \{3S_z^2 - S(S+1)\}. \quad (1a)$$

The first term describes the Zeeman interaction of the Gd spins \mathbf{S} with the static external magnetic field \mathbf{H} . g is the gyromagnetic tensor which has been assumed to be isotropic in the case of Gd^{3+} . The second term arises due to the axial crystal field (CF) which splits the $^8S_{7/2}$ ground state of Gd^{3+} into four doublets in zero field. b_2^0 is the axial CF parameter, that can be determined experimentally. We have assumed an axial field with a level splitting into zero field that amounts $12b_2^0$. For $\theta = 0^\circ$ the eigenvalues of equation (1) are given exactly by

$$E_m = g\mu_B H m + \frac{1}{3} b_2^0 [3m^2 - S(S+1)], \quad (1b)$$

where $S = \frac{7}{2}$ and $-\frac{7}{2} \leq m \leq +\frac{7}{2}$. The energy levels are plotted as a function of the external field in the lower frame of Fig. 1. The fine-structure spectrum is well described using a gyromagnetic factor $g = 2$ and an axial CF parameter $b_2^0 = 3.8$ GHz. The seven dipolar transitions at the resonance frequency $\nu = 9.14$ GHz are indicated and correspond satisfactorily to the observed fine-structure spectrum. The narrow resonance line with $g \sim 2$ ($H_{res} = 3.3$ kG) most probably corresponds to microwave absorption in Gd clusters.

As the spectrum at $\theta = 0^\circ$ is not intense enough to be followed up to higher temperatures, we have chosen the $\theta = 90^\circ$ orientation to investigate the temperature dependence of the linewidth. Figure 2 shows some representative ESR spectra for 0.5 at% Gd in UPt_3 for temperatures $4.2 \text{ K} \leq T \leq 51 \text{ K}$ at $\theta = 90^\circ$. An intense absorption line at low fields dominates the resonance absorption and its broadening can be followed up to higher temperatures. Model calculations of the ESR spectrum at $\theta = 90^\circ$ with the CF parameter $b_2^0 = 3.8$ GHz reveal that the low-field regime is dominated by two strong transitions at 1.2 kG ($-\frac{7}{2} \rightarrow -\frac{5}{2}$) and 1.5 kG ($-\frac{5}{2} \rightarrow -\frac{3}{2}$). A third important transition ($-\frac{3}{2} \rightarrow -\frac{1}{2}$) is predicted at 2.3 kG. Comparing these results with our experimental spectra, we assume that the intense resonance observed at 1.2 kG is the exchange-narrowed line of the first two transitions.

The linewidth ΔH of this resonance was determined in the temperature range $1.6 \text{ K} \leq T \leq 60 \text{ K}$ using two independent methods. Both, the computer fit of a Dysonian line [12] and the evaluation of the width of a single line described in detail by Peter [13], yield qualitatively the same results for samples with $x = 0.005$ and 0.02 which are shown in Fig. 3. The linewidth broadening in UPt_3 reveals the characteristic behavior of HF

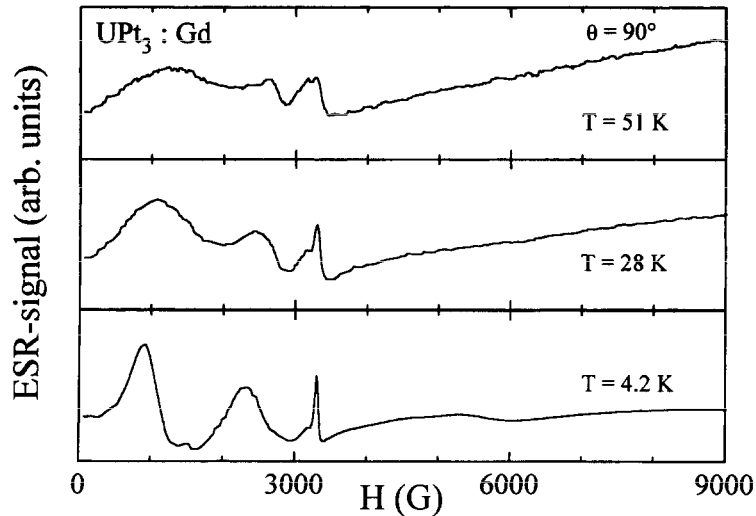


Fig. 2. Some representative Gd-ESR spectra in UPt_3 doped with 0.5 at.% Gd at temperatures 51 K (upper frame), 28 K (middle frame) and 4.2 K (lower frame). The spectra were observed using oriented powder samples with an angle of $\theta = 90^\circ$ between the crystallographic c -axis and the static external magnetic field.

systems [5]. It has been shown [11] that in HF compounds two contributions to the linewidth are important. The Korringa broadening is superimposed on contributions from spin fluctuations of the uranium moments [14]

$$\Delta H(T) = \Delta H_0 + b_n T + a T \chi_0 / \Gamma. \quad (2)$$

Here b_n is the "normal" metallic Korringa slope, χ_0 is the static magnetic susceptibility of the uranium ions and Γ the magnetic relaxation rate of the $5f$ moments. a designates the Ce-Gd coupling which is assumed to be independent of the temperature.

At very low temperatures ($T \ll T^*$) χ_0 and Γ reach constant values. Therefore we can write

$$\Delta H(T) = \Delta H_0 + b_h T, \quad (T \ll T^*), \quad (3)$$

b_h corresponds to the "heavy" low-temperature Korringa slope which is enhanced as a consequence of the large density of states. The coefficient of the Korringa slope (b_n or b_h) depends quadratically on the density of states at the Fermi energy, $N(E_F)$.

The solid line in Fig. 3 has been calculated using equation (2). Here the static susceptibility was described

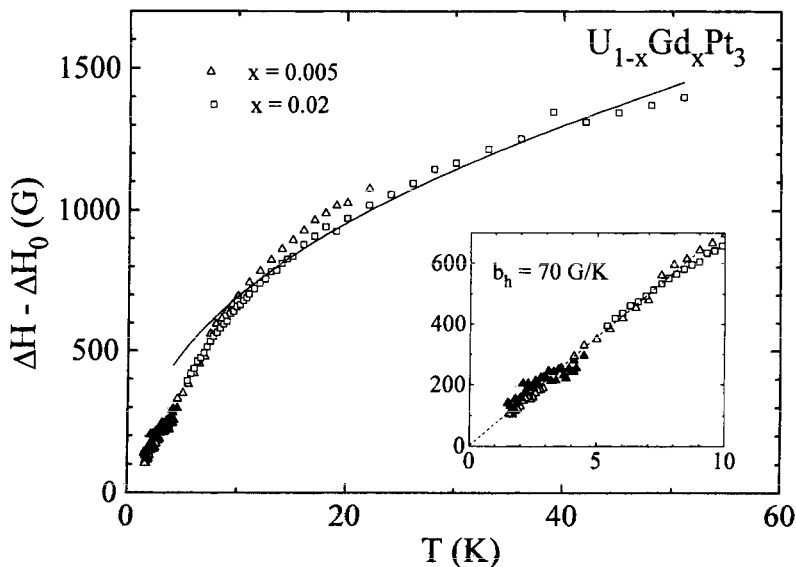


Fig. 3. Temperature dependence of the linewidth as observed in $\text{U}_{1-x}\text{Gd}_x\text{Pt}_3$. A residual linewidth $\Delta H_0 = 150$ G (300 G) has been subtracted for $x = 0.005$ (0.02). Open symbols: computer fit; full symbols: method proposed by Peter [13]. The solid line has been calculated as described in the text. The inset shows the low-temperature behavior of the linewidth. The dashed line indicates a linear Korringa dependence of 70 G K^{-1} .

using a Curie–Weiss behavior with a Curie–Weiss temperature $\theta \approx -70$ K, a characteristic temperature $T^* \approx 46$ K and a Korringa slope $b_n = 12 \text{ G K}^{-1}$. We have explicitly used a square-root temperature dependence of the magnetic relaxation rate Γ [15]. The solid line in Fig. 3 gives a reasonable fit to the experimental results, even for temperatures well below T^* . A linear temperature dependence of ΔH is observed at the lowest temperatures below 10 K. The inset shows $\Delta H(T)$ for temperatures $1.5 \text{ K} \leq T \leq 10 \text{ K}$. The solid line represents a low-temperature Korringa slope in the HF state, $b_n = 70 \text{ G K}^{-1}$, which is approximately six times enhanced compared to b_n .

No indications of the magnetic phase transition at $T_N = 5 \text{ K}$ [9] can be detected. This observation allows to conclude that (i) UPt_3 reveals no significant opening of a gap in the density of states due to the formation of a spin-density wave (SDW) and (ii) that no magnetic order of reasonable large magnetic moments ($\sim 1 \mu_B$) is established. And indeed, an ordered moment of $0.02 \mu_B$ has been determined in neutron-scattering experiments [9].

3. DISCUSSION AND CONCLUDING REMARKS

The main result of this contribution is that the Gd-ESR in UPt_3 reveals the characteristics of magnetic relaxation in heavy-fermion compounds: on decreasing temperatures the Korringa slope increases continuously due to moment compensation and the creation of heavy quasiparticles. This finding is in contrast to earlier ESR-results on UPt_3 [2]. However, the increase by a factor of six is a small effect compared to the increase in the DOS as determined in the bulk experiments. If the heavy electrons would have a pure band character the enhancement of the Korringa slope would be of the order 10^4 . The ESR results demonstrate that the low-lying excitations in heavy fermions have predominantly local character and that the heavy-electron magnetic moments reside at the $5f$ sites rather distant from the ESR probe. The dominant coupling was proposed to be via conduction-electron-mediated (RKKY-type) interactions [16]. This is important, if we compare our results to the temperature dependence of the longitudinal relaxation rate $1/T_1^{\text{NMR}}$ as obtained in NMR experiments [17]. For ESR in metals the spin–lattice relaxation time T_1^{ESR} equals the spin–spin relaxation time T_2^{ESR} which determines the ESR-linewidth $\Delta H \sim 1/T_2^{\text{ESR}}$. Hence we can compare the ESR-linewidth ΔH to the NMR-relaxation rate $1/T_1^{\text{NMR}}$ of the ^{195}Pt -nuclear spin. Cox [15] pointed out, that the f – f separation in most inter-metallic compounds is larger than the distance between the f -ions and the NMR probe sites. Due to the significant dependence on distance of the proposed interaction,

NMR probes are more sensitive to the mass enhancement compared with ESR probes. Above 0.5 K, $1/T_1^{\text{NMR}}$ follows a linear dependence indicating Fermi-liquid behavior. For $T > 7 \text{ K}$, $1/T_1^{\text{NMR}}$ reveals a tendency to saturate. These results are qualitatively similar to our observations of $\Delta H(T)$ at low temperatures (see inset in Fig. 3).

Neither in $\Delta H(T)$ nor in $1/T_1^{\text{NMR}}$ any indications of the antiferromagnetic phase transition of $T_N = 5 \text{ K}$ can be detected. This observation is in clear distinction to the results in URu_2Si_2 . In this HF compound the onset of the SDW state and the opening of a partial gap in the electronic density of states clearly can be detected in both, ESR [7] and NMR [18] experiments. From the absence of any anomaly in UPt_3 we can conclude that no gap opens in the electronic density of states and that no order of sizable localized moments is established. Even short-range magnetic order or spin-glass freezing usually can easily be detected via the linewidth broadening in ESR experiments. Hence, it seems that the onset of long-range magnetic order in UPt_3 has to be described in terms of a Stoner-like mechanism involving only a marginal fraction of electrons at the Fermi surface.

In conclusion, UPt_3 reveals the characteristic relaxation dynamics of HF systems. However, the Kondo-like excitations are strongly of local character and the increase of the DOS with decreasing temperatures is much less than observed in heat-capacity experiments and also smaller than in NMR experiments. This dependence of the mass enhancement on the distance from the probe site has been predicted by Cox [16]. The relaxation rates are not affected by the onset of magnetic order, indicating that if at all only a marginal fraction of the DOS is involved in the magnetic phase transition.

Acknowledgements—This research was partly supported by the SFB 252 and by the Bundesministerium für Bildung und Forschung (BMBF) under the contract number 13N6917/0.

REFERENCES

1. Gandra, F., Schultz, S., Oseroff, S.B., Fisk, Z. and Smith, J.L., *Phys. Rev. Lett.*, **55**, 1985, 2719.
2. Gandra, F., Pontes, M.J., Schultz, S. and Oseroff, S.B., *Solid State Commun.*, **64**, 1987, 859.
3. Grewe, N. and Steglich, F., *Handbook on the Physics and Chemistry of Rare Earth* (Edited by K.A. Gschneider Jr. and L. Eyring), Vol. 14, p. 343, 1991.
4. Stewart, G.R., *Rev. Mod. Phys.*, **56**, 1984, 755.
5. Elschner, B. and Loidl, A., *Handbook on the Physics and Chemistry of Rare Earth* (Edited by K.A. Gschneider, Jr. and L. Eyring), Vol. 24, 1997 (in print).
6. Schlott, M., Elschner, B., Herrmann, M. and ABmus, W., *Z. Physik*, **B72**, 1988, 385.

7. Spitzfaden, R., Loidl, A., Park, J.G. and Coles, B.R., *J. Phys. C: Condens. Matter.*, **8**, 1996, 2857.
8. Stewart, G.R., Fisk, Z., Willis, J.O. and Smith, J.L., *Phys. Rev. Lett.*, **52**, 1984, 679.
9. Aeppli, G., Bucher, E., Broholm, C., Kjems, J.K., Baumann, J. and Hufnagel, J., *Phys. Rev. Lett.*, **60**, 1988, 615.
10. Lee, M., Moores, G.F., Jong, Y.-Q. and Halperin, W.P., *Phys. Rev.*, **B48**, 1993, 7392.
11. Abragam, A. and Bleaney, B., *Electron Paramagnetic Resonance of Transition Ions*. Clarendon Press, Oxford, 1970.
12. Dyson, F.J., *Phys. Rev.*, **98**, 1955, 349.
13. Peter, M., *J. Appl. Phys. Suppl.*, **32**, 1961, 338.
14. Coldea, M., Schaeffer, H., Weissenberger, V. and Elschner, B., *Z. Physik.*, **B68**, 1987, 25.
15. Cox, D.L., Bickers, N.E. and Wilkins, J.W., *J. Magn. Magn. Mater.*, **54-55**, 1986, 333.
16. Cox, D.L., *Phys. Rev.*, **B35**, 1987, 6504.
17. Kohori, Y., Shibai, H., Kohara, T., Oda, Y., Kitaoka, Y. and Asayama, K., *J. Magn. Magn. Mater.*, **76&77**, 1988, 478.
18. Kohara, T., Kohori, Y., Asayama, K., Kitaoka, Y., Maple, M.B. and Torikachvili, *Solid State Commun.*, **59**, 1986, 603.